

# Numerical scheme based on the Riemann solver problem applied to protoplanetary disks

Tarik Chakkour

LGPM, CentraleSupélec, University of Paris-Saclay,

21 October 2022

# Outline

- 1 Modeling a Keplerian flow in two-phase
- 2 The conservation laws
- 3 The finite volume method in one-phase
- 4 Numerical simulations
- 5 Conclusions and perspectives



## Formation of planets in a Keplerian disk

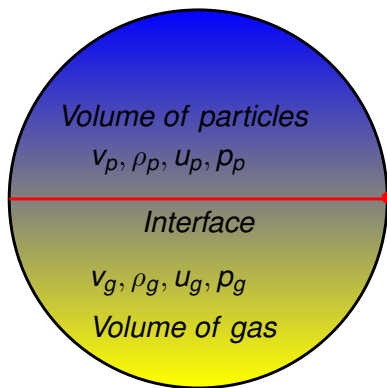


**Figure:** Modeling of two-phase flow.



## Formation of planets in a Keplerian disk

- Assuming that the disk is at hydrostatic equilibrium along the  $z$ -axis. Denoting  $\Phi$  the gravitational potential, the equilibrium hydrostatic equation involving the pressure  $p$  is given by:

$$\overrightarrow{\text{grad}}(p) = -\rho \cdot \overrightarrow{\text{grad}}(\Phi), \quad (1)$$

- $\Phi$  can be determined over the  $z$ -axis by the following equality:

$$\begin{aligned} \frac{1}{\rho} \frac{\partial p}{\partial z} &= \frac{\partial}{\partial z} \left( \frac{GM}{\sqrt{r^2 + z^2}} \right), \\ &= -\Omega^2 z. \end{aligned} \quad (2)$$

## Euler equations in one/two-phase

- The conservation laws involving the cylindrical coordinates are written in a bi-dimensional space:

$$\frac{\partial w}{\partial t} + \frac{1}{r} \frac{\partial r F(w)}{\partial r} + \frac{1}{r} \frac{\partial G(w)}{\partial \theta} = Q(w). \quad (3)$$

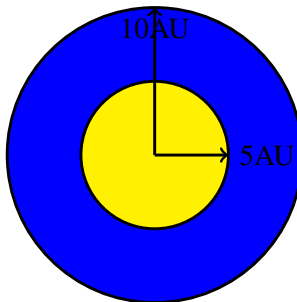
In which,  $F$  and  $G$  present respectively the fluxes in the radial and azimuthal directions, defined by:

$$F(w) = \begin{pmatrix} \rho u \\ \rho u^2 + p \\ \rho uv \\ (\rho e + p)u \end{pmatrix}, \quad G(w) = \begin{pmatrix} \rho v \\ \rho uv \\ \rho v^2 + p \\ (\rho e + p)v \end{pmatrix}, \quad Q(w) = \begin{pmatrix} 0 \\ \frac{\rho v^2}{r} - \rho \frac{GM}{r^2} + \frac{p}{r} + F_r \\ -\frac{\rho uv}{r} + F_\theta \\ -\rho u \frac{GM}{r^2} \end{pmatrix}.$$

## Computational domain

- The spatial distribution of cell is defined by the radial step  $\Delta r$  and the angular step  $\Delta\theta$  that given by:

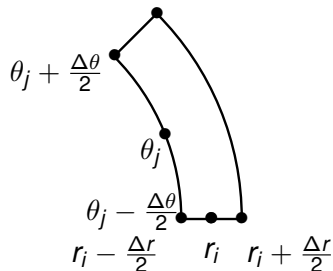
$$\begin{cases} \Delta r = \frac{r_{\text{out}} - r_{\text{in}}}{n_r}, \\ \Delta\theta = \frac{2\pi}{n_\theta}. \end{cases} \quad (4)$$



## Cylindrical cell

- The time-space complexity of the cell  $(r_i, \theta_j)$  is configured as follows:

$$\begin{cases} r_i = r_{\text{in}} + (i - \frac{1}{2})\Delta r, \\ \theta_j = (j - \frac{1}{2})\Delta\theta. \end{cases} \quad (5)$$

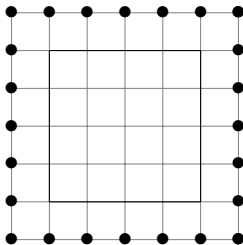


## Ghost cells

- The ghost cells provide the well-posed boundary conditions for the conservative equations, that are defined for each cell  $J_{i,j}$  by:

$$J_{i,j} = [r_{i-1/2}, r_{i+1/2}] \times [\theta_{j-1/2}, \theta_{j+1/2}]. \quad (6)$$

- The periodic boundary conditions are imposed in the azimuthal direction.





## Initial conditions

- The initial profile is previously introduced by Hayashi (1985). The density profile is calculated from the mass of planets.

$$\left\{ \begin{array}{l} \rho_{init} = \rho_0 \left( \frac{r}{r_0} \right)^{-3/2}, \\ T_{init} = T_0 \left( \frac{r}{r_0} \right)^{-1/2}, \\ p_{init} = p_0 \left( \frac{r}{r_0} \right)^{-2}, \\ u_{init} = 0, \\ v_{init} = \sqrt{\frac{GM}{r_0} (r_0/r) - 2 \frac{p}{\rho}}, \end{array} \right. \quad \left\{ \begin{array}{l} \rho_0 = 1.4 \cdot 10^{-6} \text{Kg} \cdot \text{m}^{-3}, \\ T_0 = 280 \text{K}, \\ p_0 = 1.42 \text{Pa}, \\ r_0 = 1 \text{AU}. \end{array} \right. \quad (7)$$

## Discretization

- The conservation laws defined by:

$$\partial_t \mathbf{w} + \nabla \cdot f(\mathbf{w}) = Q(\mathbf{w}). \quad (8)$$

- The integration of this equation over the control volume  $\Omega_{i,j}$  delimited by the surface  $S_{i,j}$  using Gauss's theorem gives:

$$\frac{\partial \mathbf{w}}{\partial t} \Omega_{i,j} + \int_{\partial \Omega_{i,j}} f(\mathbf{w}) d\Omega = \int_{\Omega_{i,j}} Q d\Omega. \quad (9)$$

- The discrete-time linear system is written in following form:

$$\frac{\partial \mathbf{w}_{i,j} \Omega_{i,j}}{\partial t} + \sum_l \vec{F} \cdot \vec{S} + \sum_{l'} \vec{G} \cdot \vec{S} = Q_{i,j} \Omega_{i,j}. \quad (10)$$

## Discretization

- The Taylor expansion in order 1 of pressure term is used to obtain:

$$r_{i+\frac{1}{2}} p_{i+\frac{1}{2}}^L = r_i p_i + \frac{\partial r p_i}{\partial r} \frac{\Delta r}{2} + \mathcal{O}(\Delta r^2), \quad (11)$$

$$p_{i+\frac{1}{2}}^R r_{i-\frac{1}{2}} = r_i p_i - \frac{\partial r p_i}{\partial r} \frac{\Delta r}{2} + \mathcal{O}(\Delta r^2). \quad (12)$$

- Denoting  $l$  the length of each facet, a general discretization is:

$$w_{i,j}^{n+1} = w_{i,j}^n + \Delta t \left( Q_{i,j}^n - \frac{l_{i+\frac{1}{2},j} F_{i+\frac{1}{2},j}^n - l_{i-\frac{1}{2},j} F_{i-\frac{1}{2},j}^n}{S_{i,j}^n} \right) + \Delta t \left( \frac{G_{i,j+\frac{1}{2}}^n l'_{i,j+\frac{1}{2}} - G_{i,j-\frac{1}{2}}^n l'_{i,j-\frac{1}{2}}}{S_{i,j}^n} \right). \quad (13)$$

## Discretization

- The flux terms are evaluated on the interface  $(r_{i+\frac{1}{2}}, \theta_j)$  that separates two cells  $J_{i-1,j}$  and  $J_{i,j}$  with the approximated Riemann solver  $\mathcal{H}$

$$l_{i+\frac{1}{2},j} F_{i+\frac{1}{2},j}^n = r_{i+\frac{1}{2}} \Delta\theta \mathcal{H}(w_{i+\frac{1}{2},j}^L, w_{i+\frac{1}{2},j}^R). \quad (14)$$

- For instance, considering the Godunov method, then, the conservative vector  $w$  at this interface is given as:

$$w_{i+\frac{1}{2}}^L = \begin{pmatrix} \rho_i r_{i+\frac{1}{2}} \\ u_i \\ v_i r_{i+\frac{1}{2}} \\ \rho_i r_{i+\frac{1}{2}} \end{pmatrix}, w_{i+\frac{1}{2}}^R = \begin{pmatrix} \rho_{i+1} r_{i+\frac{1}{2}} \\ u_{i+1} \\ v_{i+1} r_{i+\frac{1}{2}} \\ \rho_{i+1} r_{i+\frac{1}{2}} \end{pmatrix}. \quad (15)$$

## Discretization

- The conservative equation is resolved by a splitting extrapolation method. It allows to give the following equivalent system:

$$\begin{cases} \frac{\partial w}{\partial t} + \frac{1}{r} \frac{\partial r F(w)}{\partial r} = Q(w), \\ \frac{\partial w}{\partial t} + \frac{1}{r} \frac{\partial G(w)}{\partial r} = Q(w). \end{cases} \quad (16)$$

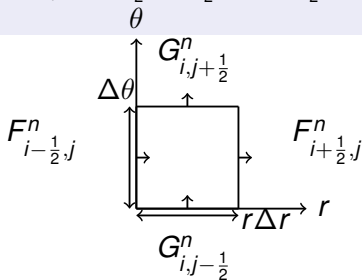
- The azimuthal flux  $G$  is approached by a cell-centred scheme with keeping the same undimensional radial flux  $F$ . The Taylor-Young expansion in points  $(r_i, \theta_j + \frac{\Delta\theta}{2})$  and  $(r_i, \theta_j - \frac{\Delta\theta}{2})$  gives:

$$\frac{G_{i,j+\frac{1}{2}} - G_{i,j-\frac{1}{2}}}{\Delta\theta} = \frac{\partial G}{\partial \theta} + \mathcal{O}((\Delta\theta)^2). \quad (17)$$

## Discretization

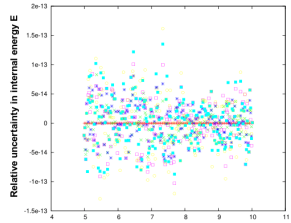
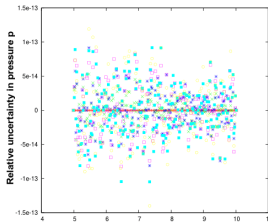
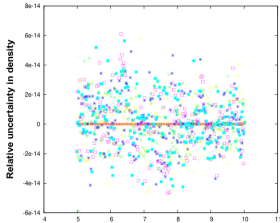
- The second-order discretization for the flux  $G$  is defined as follows:

$$G_{i,j+\frac{1}{2}} = \begin{pmatrix} \rho_{i,j+\frac{1}{2}} v_{i,j+\frac{1}{2}} \\ \rho_{i,j+\frac{1}{2}} u_{i,j+\frac{1}{2}} v_{i,j+\frac{1}{2}} \\ \rho_{i,j+\frac{1}{2}} v_{i,j+\frac{1}{2}}^2 + p_{i,j+\frac{1}{2}} \\ (\rho_{i,j+\frac{1}{2}} \mathbf{e}_{i,j+\frac{1}{2}} + p_{i,j+\frac{1}{2}}) v_{i,j+\frac{1}{2}} \end{pmatrix}.$$



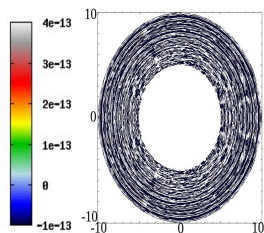
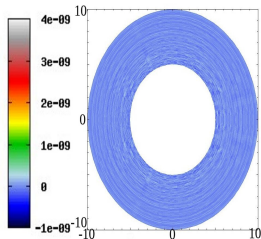
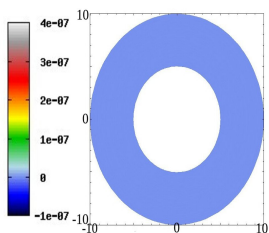
# Relative error

- The estimated relative error is stated in some physical variable. This error shows perturbation analysis in density, pressure and internal energy as shown:



## Regime steady-state

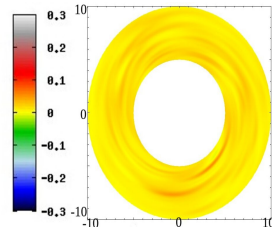
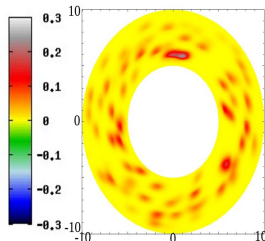
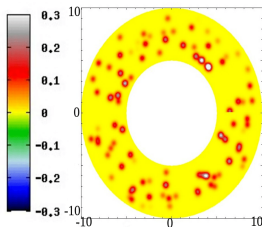
- The code accuracy is tested with computing the stationary solutions that remain uniform over time with good precision.





## Stability and long-term evolution

- The perturbation of the vortices is studied in the disk with neglecting the turbulence effects,



## Three-dimensional finite volume method

- The system of Euler equations is extended from bidimensional space to three-dimensional:

$$\frac{\partial w}{\partial t} + \frac{1}{r} \frac{\partial r F(w)}{\partial r} + \frac{1}{r} \frac{\partial G(w)}{\partial \theta} + \frac{1}{r} \frac{\partial H(w)}{\partial z} = Q(w). \quad (18)$$

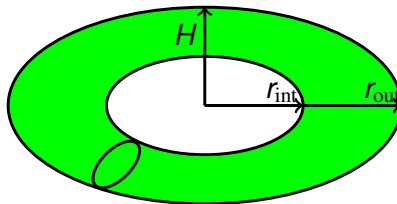


**Figure:** Computational domain in 3D.

## Conclusions

- Develop in a second-order well-balanced scheme for the compressible Euler equations with keeping the gravitational source term.
- Numerical tests will be performed by comparing the accuracy and efficiency of the new multi-slopes methods with the first order method.

**Thank  
you**